Effects of antecedent soil water content on infiltration and erosion processes on loessial slopes under simulated rainfall

Lan Ma, Junyou Li and Jingjing Liu

ABSTRACT

Soil texture and antecedent soil water content (ASWC) are primary factors governing hillslope hydrological and erosion processes. We used simulated rainfall to investigate the runoff and erosion processes on sloped plots with three loessial soils and analyzed the effects of soil texture and ASWC on the hydrological processes. The results demonstrated that the average infiltration rate decreased with increasing clay content (i.e., Ansai (AS) loamy sand > Fuxian (FX) clay loam > Yangling (YL) clay). ASWC had little effect on infiltration processes for the YL clay but exerted a significant influence on infiltration for the FX and AS soils; this implies that infiltration models for loamy soils must consider the effects of ASWC. The Horton model was found to describe infiltration processes in these loessial soils better than the Kostiakov or Philip models. The YL clay yielded much less sediment than the FX and AS soils, and its sediment yield rate gradually decreased with the rainfall duration. There was a negative relationship between clay content and sediment yield under high ASWC, but no clear relation under low ASWC. These erosion differences derived from the splash erosion for the YL clay, and the depressions or rills occurred on the loamy soil plots.

Key words | antecedent soil water content, erosion, infiltration, simulated rainfall, soil texture

Lan Ma (corresponding author)
Junyou Li
Jingjing Liu
Key Laboratory of State Administration of Forestry and Grassland on Soil and Water Conservation, School of Soil and Water Conservation,
Beijing Forestry University,
Beijing 100083,
China
E-mail: *mlpcz@sina.com*

INTRODUCTION

The Loess Plateau of China has an arid to semi-arid climate and has long experienced severe soil erosion due to its erodible soil texture, steep hillslopes, and frequent rain storms (Tang 2004). In fact, in some regions of steep terrain within the plateau, soil loss rates reach up to 5,000–10,000 Mg km^{-2} a^{-1}; such pronounced soil loss causes severe nutrient loss, induces widespread land degradation, and results in frequent severe flooding along the Yellow River (Fu *et al.* 2006). In arid and semi-arid areas, soil moisture plays an important role in sustaining vegetation growth. In particular, antecedent soil water content (ASWC) affects runoff generation and related soil erosion processes. Infiltration, runoff, and erosion processes within the Loess Plateau have been investigated previously to help conserve and use scarce soil and water resources across the region (Pan *et al.* 2006, 2016; Wei *et al.* 2014; Mei *et al.* 2018).

Soil infiltration processes under natural rainfall conditions are complex, owing primarily to spatiotemporal variability in soil properties and rainfall (Geiger & Durnford 2000; Dong *et al.* 2017). Typically, soil infiltration processes are investigated by subjecting disturbed or undisturbed soil columns to a stable hydraulic head or simulated rainfall; the infiltrated water volume and the development of the

doi: 10.2166/nh.2020.013

wetting front are commonly recorded (Youngs 1991). These soil column tests, particularly being subjected to ponding hydraulic heads, only focus on a hydrological point, in contrast to soil infiltration processes that occur on field hillslopes during rainfall events (Boers *et al.* 1992).

Soil texture tends to become coarser from south to north on the Loess Plateau, while precipitation decreases from 600 to 200 mm a^{-1} (Tang 2004). Such differences in soil texture and precipitation have a pronounced effect on ASWC and erosion processes on hillslopes (Lado *et al.* 2004). Numerous well-established soil infiltration models have been reported previously, including the Horton, Philip, and Green–Ampt models. Both the selection of an appropriate model and the quantification of model parameters are necessary to describe hillslope rainfall–runoff processes. Previous studies have conducted soil column tests to elucidate the effects of soil properties or ASWC on infiltration processes (Marcus *et al.* 2011; Makoto *et al.* 2019), and it is worth further comparing these findings of such previous studies with infiltration processes on sloped plots under rainfall conditions.

The Universal Soil Loss Equation (USLE) and the Water Erosion Prediction Project (WEPP) model are two popular predictive models for soil erosion. Soil erodibility (K) is an important factor in the USLE and is typically assessed based on soil texture (Wischmeier & Mannering 1969). Extensive field studies have been conducted by Simanton *et al.* (1987) and Elliot *et al.* (1989) to develop methods of predicting erodibility for cropland and rangeland soils based on soil properties for use in the WEPP model. Nevertheless, as Laflen (2000) suggested, the future expansion of databases detailing soil properties will be essential for continued verification of predictive models. In particular, establishing a relationship between sediment yield and soil texture will be important for the development and verification of such models.

For a sloped plot, overland flow occurs when rainfall intensity exceeds soil infiltration capacity. Soil erosion processes are controlled primarily by soil erodibility and rainfall–runoff–erosion dynamics, including raindrop splash and overland flow scour (Vermang *et al.* 2009). When soil detachment is controlled primarily by overland flow, detachment rates tend to decrease with increasing soil clay content (Wischmeier & Mannering 1969). However, the infiltration of rainfall into soils is typically greater for soils with more coarse particles than for those with finer particles under the same rainfall conditions. ASWC has an important impact on both rainfall–runoff and soil erosion processes, yet little information is available regarding the effects of ASWC on the relationship between soil texture and erodibility.

The primary objectives of the present study are as follows: (1) to evaluate the effectiveness of three infiltration models and (2) to investigate the differences in infiltration and erosion processes between the three loessial soils. The results presented here will form a useful dataset for the future assessment of soil erodibility and will help provide theoretical guidance for erosion control in the loess area.

DATA AND METHODS

Experimental set-up

Experiments were conducted in an indoor rainfall simulator with a side-sprinkle rainfall set-up. With this set-up, rainfall intensity could be controlled by adjusting spray nozzle size and water pressure, and rainfall uniformity exceeded 85%. The fall height of raindrops was approximately 16 m, which ensured kinetic energy similar to that of natural rainfall.

Six experimental plots were constructed, each with length, width, and depth of 2.00, 0.55, and 0.35 m, respectively; the plot size was selected considering the size of a standard field runoff plot (5×20 m) and avoiding marginal effects. The plots were constructed using steel, with small holes at the bottoms of the plots to allow soil water percolation. The experimental slope was adjusted to 10°; this is a common gradient for cultivated farmlands in the Loess Plateau of China. The tested soils were taken from Ansai County (AS, 36°52′N, 109°19′E), Fuxian County (FX, 35°53′N, 108°36′E), and Yangling District (YL, 34°16′N, 108°05′E), which are located along the north to south of the Loess Plateau of China. The particle size distributions of these soils are presented in Figure 1. The contribution by the weight of clay particles (<2 μm) to the total soil weight was 28%, 20%, and 12% for YL, FX, and AS soils, respectively. The YL, FX, and AS soils belong to the clay

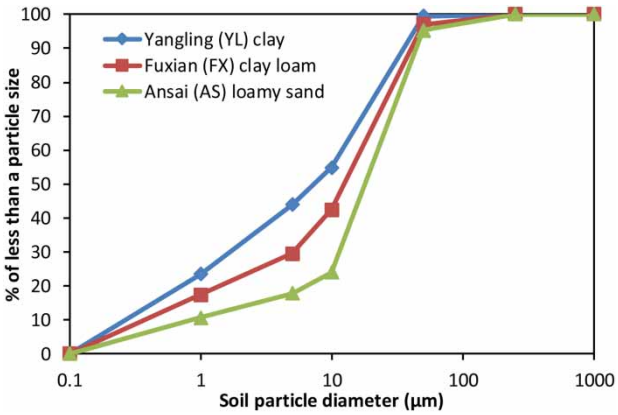

Figure 1 | Particle size distributions for tested soils.

soil, clay loam soil, and loamy sand categories, respectively, according to the international soil texture classification system (Hillel 1982).

The soils were gently crushed before being screened with a 10 mm sieve. In each plot, the soil was packed into three layers with a thickness of 10 cm and a total depth of 30 cm and a soil density of 1.20 g cm^{-3}. To avoid discontinuities between neighboring layers in each plot, each soil layer was lightly raked before the next soil layer was packed. The outlet of each plot was constructed like a shutter, with eight steel sheets (0.55×0.02 m) attached to each plot at intervals of 2 cm. Rainfall I was simulated for a dry run with low ASWC (approximately 0.13 m^3 m^{-3}). Rainfall II was applied 3 days after Rainfall I in the same soil plots for a wet run with high ASWC (0.3–0.4 m^3 m^{-3}).

Data measurement and analysis

Both rainfalls with the intensity of about 100 mm h^{-1} were administered for about 70 min, in line with typical storm characteristics for the Loess Plateau. Two replicates of each treatment were subjected to the simulated rainfall simultaneously. The time until runoff initiation was recorded for each treatment; after runoff initiation, runoff and sediment were collected for each test at 3-min intervals throughout the rainfall event. When sediment had been deposited enough, the sediment was separated from water, oven dried for 24 h at 105 °C, and weighed. Infiltration rates were calculated by subtracting the measured runoff rates from the rainfall intensity. The average sediment concentration was determined as the ratio of the total dry sediment mass collected to the total runoff volume, and the runoff coefficient was determined as the ratio of surface runoff to corresponding rainfall.

A soil's instantaneous infiltration rate (f_i) can be calculated according to the following formula (Pan *et al.* 2006):

$$f_i = I\cos\theta - \frac{10R_i}{St} \tag{1}$$

where I is rainfall intensity (mm min^{-1}), θ is slope gradient (°), t is the time interval required to collect the runoff sample (min), R_i is the runoff collected during the ith time interval (mL), and S is the area of the plot (cm^2).

In empirical infiltration models, the Kostiakov equation is typically used to describe infiltration processes in experimental soils (Kostiakov 1932):

$$f(t) = i_0 t^{-a} \tag{2}$$

where $f(t)$ is the instantaneous infiltration rate (mm min^{-1}), i_0 is the initial infiltration rate (mm min^{-1}), t is the duration (min), and a is an empirical parameter associated with soil texture.

Here, physically based models including the Horton and Philip models were selected to discuss infiltration processes for the three soils considered. The Horton equation can be written as follows (Horton 1941):

$$f(t) = f_c + (f_0 - f_c)e^{-\alpha t} \tag{3}$$

where $f(t)$ is the instantaneous infiltration rate (mm min^{-1}), f_c is the ultimate infiltration capacity or stabilized infiltration rate (mm min^{-1}), f_0 is the initial infiltration rate (mm min^{-1}), t is the duration (min), and α is the decay parameter. The parameters f_c and α depend primarily on soil properties and antecedent moisture. This equation assumes ponding conditions for the soil throughout the infiltration process due to the generation of overland runoff.

Philip (1969) suggested that soil infiltration rates decrease with time according to a power-law equation and

can be expressed as follows:

$$f(t) = A + \frac{1}{2}St^{-0.5} \quad (4)$$

where A is the constant infiltration rate (cm min^{-1}), t is the duration (min), and S is the soil suction wetting rate (cm min$^{-0.5}$), which can be obtained by fitting the cumulative infiltration amount and $t^{0.5}$ at the beginning of infiltration. This equation assumes ponding infiltration into deep soil with uniform antecedent water content.

Analysis of variance (ANOVA) and paired t-tests were used to analyze possible differences in soil infiltration and sediment yield processes between the three soils and between high and low ASWC. Correlation and regression analyses were also undertaken to investigate the relationship between sediment yield and runoff. The above analyses were performed using SPSS 19.0 (by SPSS Inc., an IBM Company).

RESULTS AND DISCUSSION

Runoff and infiltration

Under low ASWC conditions (0.13 m^3 m^{-3}; Rainfall I), the average infiltration rates for the YL clay, FX clay loam, and AS loamy sand were 0.34, 0.66, and 0.97 mm min^{-1}, respectively. Significant differences between the three soils were found at the $p = 0.05$ level (Table 1). The runoff coefficients for the different soil types decreased in the following order: YL clay (0.80) > FX clay loam (0.56) > AS loamy sand (0.40).

Under high ASWC (0.30–0.40 m^3 m^{-3}; Rainfall II), the average infiltration rates and runoff coefficients for the three soils were 0.31–0.50 mm min^{-1} and 0.71–0.81, respectively. The AS loamy sand had a higher average and stabilized infiltration rate than the YL clay and FX clay loam, and there was no significant difference ($p = 0.05$) between the YL clay and FX clay loam (Table 1). The average and stabilized runoff coefficients for the three soil types decreased in the following order: YL clay (0.81) > FX clay loam (0.78) > AS loamy sand (0.71). These results demonstrate that soil infiltration rates increase as clay content decreases and indicate that the runoff coefficient decreases with decreasing clay content under similar rainfall conditions. This is in accordance with previous findings based on soil column tests (Makoto *et al.* 2019).

Based on the comparison between Rainfall I and II, ASWC had no significant effect ($p = 0.05$) on the average infiltration rate and runoff coefficient for the YL clay. This behavior is similar to that reported by Benito *et al.* (2003), who demonstrated little difference in runoff or soil infiltration rates between dry and wet periods for clay soils. This can be attributed to the low porosities typical of clay soils. In contrast, the infiltration rates for the AS loamy sand and FX clay loam under low ASWC were both about two times greater than those under high ASWC. This result agrees with both Cerdà (1996) and Jones (1997), who found that field soils with sandy or loamy characteristics exhibit significantly greater infiltration rates during dry periods than during wet periods.

Table 1 | Runoff, infiltration, and sediment yield characteristics for YL clay, FX clay loam, and AS loamy sand plots under low and high ASWC

		The average value during the rainfall process				The stabilized value[a]			
Soil	ASWC (m^3 m^{-3})	IR	RC	SYR	SC	IR	RC	SYR	SC
YL	0.13	0.34 a[b]	0.80 a	5.13 a	3.76 a	0.27 a	0.84 a	2.04 a	1.43 a
FX	0.13	0.66 b	0.56 b	9.26 b	11.21 b	0.40 b	0.73 b	9.68 b	9.07 b
AS	0.13	0.97 c	0.40 c	2.37 c	3.77 a	0.80 c	0.56 c	1.88 a	2.11 a
YL	0.30	0.31 a	0.81 a	4.36 a	3.30 a	0.31 a	0.81 a	2.44 a	1.86 a
FX	0.35	0.34 a	0.78 a	32.72 b	27.36 b	0.25 a	0.86 a	12.75 b	9.70 b
AS	0.40	0.50 b	0.71 b	35.69 c	29.76 c	0.43 b	0.75 b	–	–

IR, infiltration rate (mm min^{-1}); RC, runoff coefficient; SYR, sediment yield rate (g m^{-2} min^{-1}); SC, sediment concentration (kg m^{-3}).

[a]The average of the last four observed values during the later phase of rainfall.

[b]The same letter represents no significant differences at the $p = 0.05$ level among the three soil using ANOVA.

The stable infiltration rates and runoff coefficients attained at the later stage of rainfall exhibited variation similar to that observed for the average values presented in the preceding paragraph. Significant differences in these parameters between low and high ASWC conditions were found for the FX clay loam and AS loamy sand, but not for the YL clay. These results provide further evidence that ASWC likely has little effect on clay soils but has a significant effect on loamy or sandy soils.

For the three soils considered, the cumulative infiltration volume ($F(t)$) increased with rainfall duration; this relationship can be described well by the power-law equation $F(t) = at^b$ (Figure 2 and Table 2). The exponent b in the regressed equations was found to be in the ranges 0.52–0.77 and 0.74–0.83 for low and high ASWC, respectively; moreover, values of b were found to increase with decreasing clay content. The regressed power equations were converted into logarithmic lines, and the differences between the three soil types were further analyzed. Under low ASWC, significant differences ($p = 0.05$) in cumulative infiltration processes were found between the three soils; under high ASWC, the AS loamy sand exhibited a significantly higher infiltration volume than both the FX clay loam and YL clay. Low ASWC generated a greater infiltration volume than high ASWC for both FX clay loam and AS loamy sand. In contrast, the cumulative infiltration volume varied little between low and high ASWC for the YL clay (Figure 2 and Table 1), although the low ASWC corresponded to a higher a-value in the regressed equations. This indicates that, for clay soils, ASWC may have a greater influence on initial infiltration processes than later period.

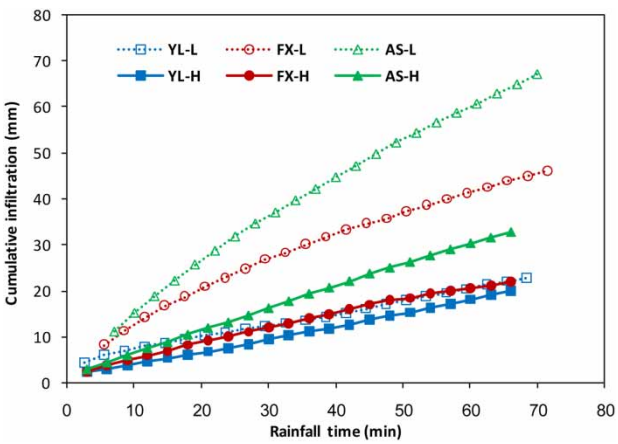

Figure 2 | Cumulative infiltration processes for YL clay, FX clay loam, and AS loamy sand plots under low (L) and high (H) ASWC.

Changes in the infiltration rate throughout the simulated rainfall event are shown in Figure 3 for all three soils and both low and high ASWC. Under low ASWC conditions (Rainfall I), overland sheet flow occurred 2.5, 5, and 7 min after the initiation of simulated rainfall for the YL clay, FX clay loam, and AS loamy sand, respectively. The infiltration rate for the YL clay decreased quickly to reach 0.3 mm min^{-1} after the initial 8.5 min and then stabilized; conversely, the infiltration rate decreased continuously throughout the rainfall duration for both the FX clay loam and AS loamy sand. However, under high ASWC conditions, the infiltration rates of all three soils decreased abruptly, with all soil types reaching stable values within 10 min.

The Kostiakov, Horton, and Philip models were adopted to fit the infiltration processes illustrated in Figure 3 using the least square method (Table 3).

Table 2 | Best-fit equations for relationship between cumulative infiltration volume ($F(t)$), cumulative sediment yield ($S(t)$), and rainfall time (t) for soils considered under low and high ASWC

			$F(t)$		$S(t)$	
ASWC (m^3 m^{-3})	Soil	Number	The best-fit equation	R^2	The best-fit equation	R^2
0.13	YL	23	$F(t) = 2.290t^{0.517}$	0.974	$S(t) = 59.970t^{0.430}$	0.949
0.13	FX	23	$F(t) = 2.719t^{0.668}$	0.998	$S(t) = 0.083t^{2.145}$	0.992
0.13	AS	22	$F(t) = 2.619t^{0.767}$	0.998	$S(t) = 61.61\ln(t) - 105.9$	0.967
0.30	YL	23	$F(t) = 0.741t^{0.760}$	0.978	$S(t) = 43.850t^{0.446}$	0.995
0.35	FX	23	$F(t) = 0.968t^{0.743}$	0.998	$S(t) = 800.50\ln(t) - 1{,}202.0$	0.971
0.40	AS	23	$F(t) = 0.981t^{0.829}$	0.995	$S(t) = 88.68e^{0.051t}$	0.965

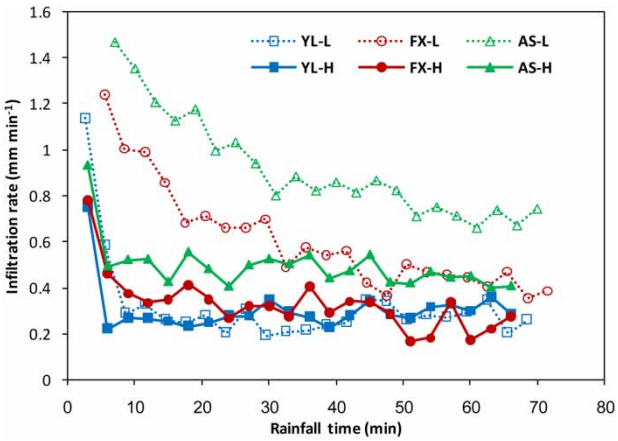

Figure 3 | Infiltration rates vs. rainfall time for YL clay, FX clay loam, and AS loamy sand plots under low (L) and high (H) ASWC.

Based on the coefficient of determination (R^2), the Kostiakov model can describe infiltration processes better for the FX clay loam and AS loamy sand than for the YL clay. The i_0-values in the Kostiakov model were found to vary in the ranges 0.77–2.93 and 0.62–1.0 mm min^{-1} for low and high ASWC, respectively. Moreover, the FX clay loam and AS loamy sand exhibited significantly higher i_0-values than the YL clay. This finding supports the assertion that initial infiltration rates decrease with increasing clay content.

The Horton model can give both initial (f_0) and stabilized infiltration rates (f_c). For the three soils, the fitted f_c-values were found to decrease with increasing clay content and were close to the observed values (Tables 1 and 3). The fitted f_0-values of the three soils were in the ranges 1.50–2.51 and 1.44–1.75 mm min^{-1} under low (Rainfall I) and high ASWC (Rainfall II), respectively. The AS loamy sand and YL clay were found to have greater f_0-values than the FX clay loam. The greater f_0-value obtained for the YL clay may be related to the abrupt decline in the infiltration rate during the initial phase of rainfall (Figure 3).

The parameters A and S in the Philip model represent the stabilized and initial infiltration rates, respectively. Both A and S increased with increasing clay content. However, the Philip model generated a significantly lower stabilized and initial infiltration rate than the Horton model (i.e., $A < f_c$ and $S < f_0$; Table 3).

Under the simulated rainfall conditions, it was difficult to accurately observe the initial soil infiltration rate owing to the relatively low rainfall intensity. However, the Horton model produced stabilized infiltration rates (f_c) that were close to the observed values (Tables 1 and 3), and higher R^2 values were obtained for the Horton model than the Kostiakov and Philip models. These results suggest that the Horton model is more suited than the Kostiakov or Philip models to describing the infiltration processes of loessial soils under the rainfall conditions considered here. Zhao *et al.* (2009) found that both the Horton and Philip models can describe soil infiltration processes well for the loessial soils of the Loess Plateau based on soil column tests. Additionally, Genachte *et al.* (1996) conducted experiments on the soil infiltration behaviors of Arenosol and Ferralsol soils in tropical rain forests and suggested that the effectiveness of infiltration models depends partly on soil properties. In particular, Genachte *et al.* (1996) found that the Philip and Horton models could describe infiltration processes for the Arenosol better than the Kostiakov model, while all of the models considered (i.e., Philip, Kostiakov, and

Table 3 | Fitted infiltration models for YL clay, FX clay loam, and AS loamy sand under low and high ASWC

			Kostiakov model		Horton model		Philip model	
Soil	**ASWC (m^3 m^{-3})**	**Number**	$f(t) = i_0 t^{-a}$	R^2	$f(t) = f_c + (f_0 - f_c)e^{-\alpha t}$	R^2	$f(t) = A + \frac{1}{2}St^{-0.5}$	R^2
YL	0.13	23	$f(t) = 0.772t^{-0.29}$	0.44	$f(t) = 0.262 + 2.254e^{-0.375t}$	0.94	$f(t) = 0.025 + 1.387t^{-0.5}$	0.72
FX	0.13	23	$f(t) = 2.836t^{-0.46}$	0.91	$f(t) = 0.40 + 1.096e^{-0.06t}$	0.94	$f(t) = 0.069 + 2.838t^{-0.5}$	0.94
AS	0.13	22	$f(t) = 2.934t^{-0.34}$	0.94	$f(t) = 0.675 + 1.115e^{-0.051t}$	0.96	$f(t) = 0.322 + 3.210t^{-0.5}$	0.95
YL	0.30	23	$f(t) = 0.622t^{-0.21}$	0.37	$f(t) = 0.28 + 1.471e^{-0.463t}$	0.94	$f(t) = 0.11 + 0.943t^{-0.5}$	0.77
FX	0.35	23	$f(t) = 1.017t^{-0.35}$	0.76	$f(t) = 0.293 + 1.143e^{-0.289t}$	0.91	$f(t) = 0.115 + 1.026t^{-0.5}$	0.92
AS	0.40	23	$f(t) = 0.998t^{-0.21}$	0.70	$f(t) = 0.467 + 1.261e^{-0.381t}$	0.93	$f(t) = 0.295 + 0.958t^{-0.5}$	0.88

Horton models) could predict infiltration behaviors well for the Ferralsol.

The clay contents of the YL, FX, and AS soils were approximately 28%, 20%, and 13%, respectively (Figure 1), and their corresponding average and steady infiltration rates decreased in the following order: AS > FX > YL. This provides further evidence that the soil infiltration rate decreases with increasing clay content. For both the FX and AS soils, high ASWC generated a lower steady infiltration rate; in contrast, ASWC had little effect on the infiltration rate for the YL clay (Figure 3 and Table 2). This indicates that, for soils with high clay content (i.e., >30%), ASWC has little effect on soil infiltration processes during rainfall events. However, for loamy soils (i.e., clay content <20%), infiltration models should consider the effects of ASWC. These results may reflect the higher porosity of loamy soils relative to clay soils, allowing loamy soils to both hold more water and induce greater expansion of soil volume.

Sediment yield

Cumulative sediment yields increased with rainfall duration, exhibiting power-law, exponential, or logarithmic linear distributions (Figure 4 and Table 2). The differences found in the best-fit equations indicate that sediment yield processes (or rather, change processes in sediment yield with the rainfall duration) varied with soil texture and ASWC. Under high ASWC, the AS loamy sand exhibited sediment yield behavior with an exponential distribution, with the cumulative sediment yield accelerating during the later phase of the rainfall. This behavior differs markedly from that of the other soil types (Figure 4). The YL clay exhibited similar sediment yield distributions for both high and low ASWC. In contrast, the obtained cumulative curves are markedly different under high and low ASWC for the FX and AS soils with high ASWC generating significantly greater sediment yields than low ASWC. These results indicate that the sediment yield may not be predicted effectively based on rainfall duration under different ASWC conditions.

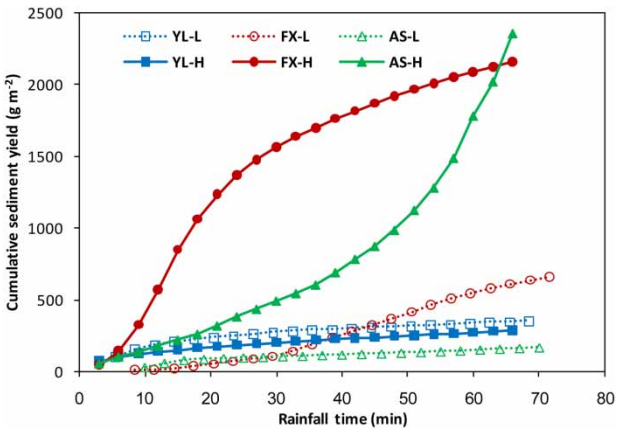

Figure 4 | Cumulative sediment yield vs. rainfall duration for YL clay, FX clay loam, and AS loamy sand plots under low (L) and high (H) ASWC.

Under low ASWC (Rainfall I), the FX clay loam plot exhibited an average sediment yield rate of 9.26 g m^{-2} min^{-1}; this value is 1.8 and 3.9 times greater than the values obtained for the YL clay and AS loamy sand, respectively. Thus, the average sediment yield rate was lowest for the AS loamy sand, likely because this soil exhibited the highest average infiltration rate (Table 1) and the lowest average runoff rate. No significant difference ($p = 0.05$) was found between the average sediment concentrations for the AS loamy sand and YL clay (Table 1). The higher sediment yield for the FX clay loam plot can be attributed to the occurrence and development of rills. In contrast, the difference in sediment yields between the AS loamy sand and YL clay can be attributed primarily to differences in soil infiltration processes. The AS loamy sand exhibited an average infiltration rate that was approximately three times greater than that of the YL clay. Therefore, the AS loamy sand plot can be considered to have had lower runoff erosion energy, even though its soil erodibility would have been higher than that of the YL clay (Wischmeier & Mannering 1969; Elliot *et al.* 1989). During the later phase of rainfall, the FX clay loam exhibited a stabilized sediment yield rate of 9.26 g m^{-2} min^{-1}, which is almost five times that obtained for the YL clay and AS loamy sand (Figure 5). These results demonstrate that differences in the sediment yield rate between the three soil types are considerably greater during the later stage of rainfall than during the earlier stage.

Under high ASWC (Rainfall II), FX clay loam and AS loamy sand exhibited similar sediment yield rates (32.7 and 35.7 g m^{-2} min^{-1}, respectively) and sediment concentrations (27.36 and 29.76 kg m^{-3}, respectively). These values are eight and nine times those of the YL clay,

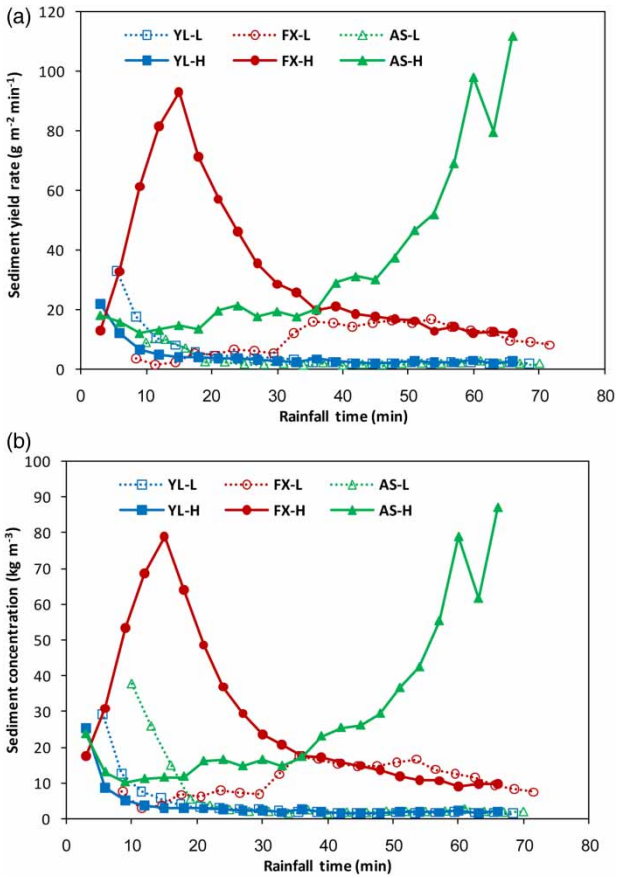

Figure 5 | (a) Sediment yield rate and (b) sediment concentration vs. rainfall duration for YL clay, FX clay loam, and AS loamy sand plots under low (L) and high (H) ASWC.

respectively (4.36 g m^{-2} min^{-1} and 3.3 kg m^{-3}) (Table 1). The greater sediment yields of the FX clay loam and AS loamy sand are in accordance with their relatively low soil erodibility compared to the YL clay. Moreover, during the later phase of rainfall, the sediment yield rates of the YL clay and FX clay loam remained relatively stable, while the AS loamy sand plot exhibited significant increases in sediment concentration and the sediment yield rate (Figure 5).

In the present study, no clear relationship was observed between clay content and sediment yield under low ASWC, although a negative relationship was observed under high ASWC (Figures 4 and 5). This could be a result of different erosional forms, and depressions or rills tended to occur on the loamy soil plots with high ASWC. For the YL and AS soils, initial sediment yield rates were greater than steady sediment yield rates under low ASWC. In contrast, initial sediment yield rates were lower than steady sediment yield rates for the FX soil; this could be attributed to the development of depressions under low ASWC for this soil type (Figure 5). Similar results have been reported previously for the YL and AS soils (Pan *et al.* 2006) and may reflect expansion and shrinkage of the surface soil layer and the greater raindrop splash during the initial rainfall stage.

The FX clay loam and AS loamy sand plots generated significantly higher sediment yields under high ASWC (Rainfall II) than under low ASWC (Rainfall I). In contrast, no clear difference in sediment yield between low and high ASWC was observed for the YL clay plot (Table 1). This suggests that ASWC has a more significant effect on loamy or sandy soils than clay soils.

Differences in sediment yield processes between low and high ASWC were considered using paired *t*-tests. No significant difference was found for the YL clay. However, high ASWC led to sediment yields that were 3.5 and 15 times higher than those under low ASWC for the AS loamy sand and FX clay loam, respectively. Benito *et al.* (2003) found sediment concentration to be greater during wet periods than dry periods for all water-repellent soil sites considered. Here, the sediment yields obtained for the AS loamy sand and FX clay loam under different ASWC support the findings of Benito *et al.* (2003), although the YL clay results do not. This highlights the importance of the effects of soil texture and ASWC on soil erosion.

Under low ASWC (Rainfall I), the sediment concentration for the FX clay loam increased gradually, reaching approximately 17.5 kg m^{-3} after 35 min, and then stabilized at 10–15 kg m^{-3} (Figure 5). This behavior may be associated with the development of rills. In contrast to the FX clay loam, both sediment yield rate and sediment concentration for the YL clay and AS loamy sand plots increased rapidly, peaking after 3 min, and then decreased slowly to reach stabilized values during the later phase of rainfall (Figure 5). No rill development was observed in the YL clay and AS loamy sand plots. This, combined with the occurrence of peak sediment yields during the initial phase of rainfall for these soils, supports the assertion that soil erosion in the YL clay and AS loamy sand plots results primarily from raindrop splash. Moreover, easily-eroded soils are typically transported during the initial phases of rainfall events,

such that their supply is exhausted by the time later runoff phases occur. This phenomenon has been observed frequently on vegetated slopes or on relatively small plots of bare soil (Pan & Shangguan 2006).

Under high ASWC (Rainfall II), notable differences in sediment yield processes were observed between the different soil types. The sediment yield rate and sediment concentration for the YL clay plot decreased gradually, while those for the AS loamy sand plot increased continuously. The decreasing trend observed for the YL clay plot can be attributed primarily to the dominance of raindrop splash erosion processes. Conversely, the continuous increase in erosion for the AS loamy sand plot can be attributed to soil collapse in the downslope area under high ASWC. Both the sediment yield rate and sediment concentration were found to increase linearly for the FX clay loam plot, peaking after 15 min, before decreasing gradually to reach a constant value. This behavior can be attributed primarily to the accelerated development of rills during the initial phase of rainfall and their relative stability during later phases.

For the YL clay, no significant difference ($p = 0.05$) in sediment yield processes was observed between low and high ASWC (i.e., between Rainfall I and II). In particular, the sediment concentration decreased rapidly from an initial peak value of 23.6–3.5 kg m^{-3} after 12 min; then, it decreased gradually to reach a stable value of 2.0 kg m^{-3} during the later stage of rainfall. However, for the FX clay loam and AS loamy sand, high ASWC (Rainfall II) yielded significantly more sediment than low ASWC (Rainfall I) (Figure 5). Although the AS loamy sand and FX clay loam yielded similar volumes of sediment overall, differences in sediment processes between these two soil types were very significant (Figure 5).

Relationship between the sediment and runoff

Under low ASWC (Rainfall I), a significant positive relationship was observed between the sediment yield rate and the runoff rate for the FX clay loam, with a correlation coefficient (R) of 0.76; conversely, a negative relationship ($R = 0.74$) was found for both the YL clay and AS loamy sand. However, under high ASWC (Rainfall II), the relatively stable runoff rate corresponded to a greater variation in the sediment yield rate (Figure 6); this likely occurred because the soil

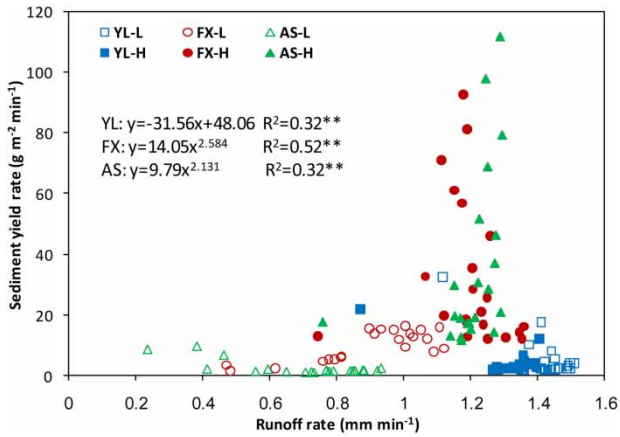

Figure 6 | Relationship between the runoff rate and the sediment yield rate for YL clay, FX clay loam, and AS loamy sand plots under low (L) and high (H) ASWC.

infiltration rate initially decreased abruptly before remaining relatively constant during the later phase of runoff (Figure 3). These different relationships under low and high ASWC indicate that ASWC has an important effect on the correlation between the runoff rate and the sediment yield rate.

When both low and high ASWC are considered together, the results presented here indicate that the sediment yield rate decreased linearly with the runoff rate for the YL clay; in contrast, higher runoff rates led to increased sediment yield rate (as described by a power-law function) for both the AS loamy sand and FX clay loam (Figure 6). In the present study, the plot surfaces were observed after each rainfall. Scattered depressions were observed for the AS and FX soils, while neither rills nor depressions were observed for the YL clay under either low or high ASWC. This suggests that raindrop splash dominates erosion processes for the YL clay, while runoff scouring likely dominates the AS and FX soils. For the YL clay, more soil particles were eroded by raindrop splash and delivered to the outlet at the beginning of the rainfall than later. Correspondingly, a negative relationship was observed between the sediment yield rate and the runoff rate for the YL clay. Previous studies have observed a similar negative relationship between erosion and the runoff rate for soils with high clay content (Pan *et al.* 2006).

Under the same runoff rates, high ASWC led to greater sediment yield rates for the FX clay loam and AS loamy sand. This can be attributed primarily to the development of rills and the collapse of the soil mass. However, for the

YL clay, low ASWC was found to generate greater sediment yield rates than high ASWC during the initial phase of rainfall for the same runoff rates. This result can be attributed to soil particles being more detachable under low ASWC.

The positive relationship between the runoff rate and the sediment yield rate for the FX clay loam and AS loamy sand plots supports a popular viewpoint that increasing the runoff rate tends to enhance the soil detachment rate owing to increases in erosional force or runoff energy (Laflen 2000). However, for the YL clay plot, increasing the runoff rate led to decreasing the sediment yield rate (Figure 6). These results suggest that inter-rill erosion dominated by raindrop splash (as occurred for the YL clay) may have little relation to overland runoff.

For a rainfall depth of approximately 100 mm, the AS loamy sand and FX clay loam plots produced approximately 82 mm of runoff under high ASWC (Rainfall II). This is significantly greater than the runoff depths generated under low ASWC (Rainfall I), which were 44 and 60 mm for the AS loamy sand and FX clay loam, respectively. Under high ASWC, the FX clay loam and AS loamy sand plot yielded 2,159 and 2,355 g m^{-2} sediments, respectively; these values are 3 and 13 times, respectively, the corresponding values observed under low ASWC (Rainfall I; Figure 7). In contrast, runoff volume and sediment yield for the YL clay varied little between low and high ASWC.

Regression analysis was undertaken to predict the relationship between cumulative sediment yield and cumulative runoff (Table 4). Generally, a linear or power-law equation

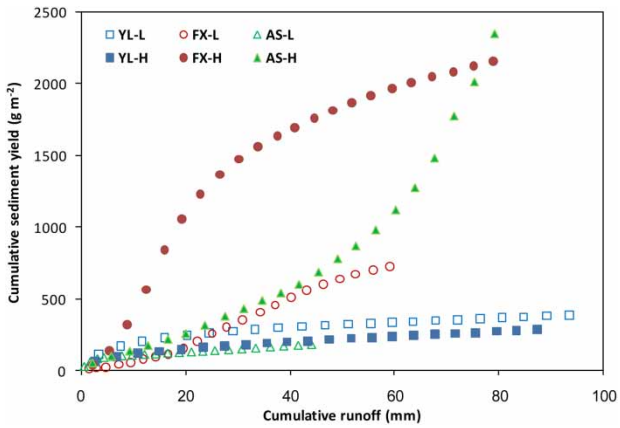

Figure 7 | Cumulative sediment yield vs. cumulative runoff for YL clay, FX clay loam, and AS loamy sand plots under low (L) and high (H) ASWC.

Table 4 | Best-fit equations between cumulative sediment yield (S) and cumulative runoff volume (R) for soils considered under low and high ASWC

ASWCs (m^3 m^{-3})	The tested soils	The best-fit equations	Number	R^2
0.13	YL clay	$S = 80.85R^{0.350}$	23	0.982
0.13	FX clay loam	$S = 13.84R - 66.68$	23	0.987
0.13	AS loamy sand	$S = 45.32R^{0.364}$	22	0.941
0.30	YL clay	$S = 45.05R^{0.408}$	23	0.998
0.35	FX clay loam	$S = 34.06\ln(R) + 36.2$	23	0.952
0.40	AS loamy sand	$S = 95.27e^{(0.042R)}$	23	0.963

was found to effectively describe this relationship, except for the FX clay loam and AS loamy sand under high ASWC (Rainfall II). For the YL clay plot, and for the AS loamy sand plot under low ASWC only, the cumulative sediment yield increased with total runoff volume and the exponent of the regressed power equation was in the range of 0.35–0.41. In this context, an exponent smaller than 1.0 indicates that the erosion rate would decrease gradually with rainfall duration. Such behavior is in line with that expected to occur when inter-rill erosion processes are dominated by raindrop splash. A linear relationship in this context indicates that the erosion rate remains relatively constant throughout the rainfall period; this is considered to be in line with the development of rill erosion within the FX clay loam plot under low ASWC (Table 4). Linear or power-law relationships between runoff and sediment load have been reported previously at the watershed scale (García-Ruiz *et al.* 2008; López-Tarazón *et al.* 2010; Tuset *et al.* 2016). However, the exponential equation obtained for the AS loamy sand plot under high ASWC indicates that the soil detachment rate accelerated gradually during the rainfall simulation; this behavior can be explained by soil collapse in the downslope area. In general, the relationship between runoff and sediment depends primarily on soil erosion processes, which in turn are controlled partly by soil texture and ASWC.

CONCLUSIONS

The simulated rainfall experiments in sloped soil plots were used to investigate the effects of soil texture and ASWC (0.13 and 0.35 m^3 m^{-3}) on infiltration and erosion

processes. The clay (<2 μm) contents of the YL, FX, and AS soils in this test corresponded to approximately 28%, 20%, and 12% by weight, respectively.

Under the same rainfall conditions, average soil infiltration rates decreased with increasing clay content. ASWC had little effect on infiltration processes for the YL clay but had significant effects for the FX and AS soils. The Horton model was found to more effectively describe infiltration processes for these three loessial soils than the Kostiakov or Philip models.

Under both low and high ASWC, the YL clay had a decreasing sediment yield rate with rainfall duration and generated much lower sediment yield than the FX and AS soils. The low sediment yield for the YL clay was mainly attributed to the dominance of raindrop splash erosion. The FX and AS soils had greater sediment yields under high ASWC than under low ASWC, which derived from the development of rills. There was no constant relationship between the sediment yield rate and the runoff rate, implying the importance of erosion form in predicting the soil erosion process on a hillslope.

ACKNOWLEDGEMENTS

This study was supported by the National Natural Science Foundation of China (Grant No. 51779004). We would like to express great gratitude to the reviewers for their valuable suggestions made to improve the manuscript.

AUTHOR CONTRIBUTIONS

L.M. conceived and designed the experiments; L.M., J.L., and J.L. performed the experiments and analyzed the data; L.M. wrote the paper.

REFERENCES

Benito, E., Santiago, J. L., Blas, D. E. & Varela, M. E. 2003 Deforestation of water-repellent soils in Galicia (NW Spain): effects on surface runoff and erosion under simulated rainfall. *Earth Surface Processes and Landforms* **28**, 145–155.

Boers, T. M., Deurzen, V. F. J. M. P., Eppink, L. A. A. J. & Ruytenberg, R. E. 1992 Comparison of infiltration rates with an infiltrometer, a rainulator and a permeameter for erosion research in S E Nigeria. *Soil Technology* **5**, 13–26.

Cerdà, A. 1996 Seasonal variability of infiltration rates under contrasting slope conditions in southeast Spain. *Geoderma* **69**, 217–232.

Dong, H., Huang, R. Q. & Gao, Q. F. 2017 Rainfall infiltration performance and its relation to mesoscopic structural properties of a gravelly soil slope. *Engineering Geology* **230**, 1–10.

Elliot, W. J., Laflen, J. M. & Kohl, K. D. 1989 *Effect of Soil Properties on Soil Erodibility*. ASAE/CSAE, St. Joseph, MI, Paper No. 89-2150.

Fu, B. J., Hu, C. X., Chen, L. D., Honnay, O. & Gulinck, H. 2006 Evaluating change in agricultural landscape pattern between 1980 and 2000 in the Loess hilly region of Ansai County, China. *Agriculture, Ecosystems & Environment* **114** (2–4), 387–396.

García-Ruiz, J. M., Regüés-Muñoz, D., Alvera, B., Lana-Renault, N., Serrano-Muela, M. P., Nadal-Romero, E., Navas-Izquierdo, A., Latrón, J., Bono, C. E. M. & Arnáez-Vadillo, J. 2008 Flood generation and sediment transport in experimental catchments affected by land use changes in the central Pyrenees. *Journal of Hydrology* **356**, 245–260.

Geiger, S. L. & Durnford, D. S. 2000 Infiltration in homogeneous sands and a mechanistic model of unstable flow. *Soil Science Society of America Journal* **64**, 460–469.

Genachte, G. V., Mallants, D., Ramos, J., Deckers, J. A. & Feyen, J. 1996 Estimating infiltration parameters from basic soil properties. *Hydrological Processes* **10**, 687–701.

Hillel, D. 1982 *Introduction to Soil Physics*. Academic Press, New York.

Horton, R. E. 1941 An approach toward a physical interpretation of infiltration-capacity 1. *Soil Science Society of America Journal* **5** (C), 399–417.

Jones, J. A. A. 1997 *Global Hydrology: Processes, Resources and Environmental Management*. Longman, Harlow.

Kostiakov, A. N. 1932 On the dynamics of the coefficient of water percolation in soils and on the necessity for studying it from a dynamic point of view for purposes of amelioration. In: *Transactions of 6th Committee International Society of Soil Science*, Russia, Part A, pp. 17–21.

Lado, M., Ben-Hur, M. & Shainberg, I. 2004 Soil wetting and texture effects on aggregate stability, seal formation, and erosion. *Soil Science Society of America Journal* **68**, 1992–1999.

Laflen, J. M. 2000 WEPP-erosion prediction technology. In: *Soil Erosion and Dryland Farming* (J. M. Laflen, J. L. Tian & C. H. Huang, eds). CRC Press, New York, pp. 557–566.

López-Tarazón, J. A., Batalla, R. J., Vericat, D. & Balasch, J. C. 2010 Rainfall, runoff and sediment transport relations in a mesoscale mountainous catchment: the River Isabena (Ebro basin). *Catena* **82**, 23–34.

Makoto, H., Heinz, G. S. & Daiki, A. 2019 Removal of saline water due to road salt applications from columns of two types of sand by rainwater infiltration: laboratory experiments and model simulations. *Water, Air, & Soil Pollution* **230**, 305.

Marcus, A. H., William, E. C., Richard, B. D., Greg, H., Shaun, L. & Kathrin, M. 2011 Effect of antecedent soil moisture on preferential flow in a texture-contrast soil. *Journal of Hydrology* **398**, 191–201.

Mei, X. M., Zhu, Q. K., Ma, L., Zhang, D., Wang, Y. & Hao, W. J. 2018 Effect of stand origin and slope position on infiltration pattern and preferential flow on a Loess hillslope. *Land Degradation & Development* **29**, 1353–1365.

Pan, C. Z. & Shangguan, Z. P. 2006 Runoff hydraulic characteristics and sediment generation in sloped grassplots under simulated rainfall conditions. *Journal of Hydrology* **331**, 178–185.

Pan, C. Z., Shangguan, Z. P. & Lei, T. W. 2006 Influences of grass and moss on runoff and sediment yield on sloped loess surfaces under simulated rainfall. *Hydrological Processes* **20**, 3815–3824.

Pan, C. Z., Ma, L. & Wainwright, J. 2016 Particle selectivity of sediment deposited over grass barriers and the effect of rainfall. *Water Resources Research* **52**, 7963–7979.

Philip, J. R. 1969 Theory of infiltration. In: *Advances in Hydro-Science, Vol. 5* (T. H. Chow, ed.). Academic Press, New York, pp. 215–296.

Simanton, J. R., Weltz, M. A., West, L. T. & Wingate, G. D. 1987 *Rangeland Experiments for Water Erosion Prediction Project*. ASAE/CSAE, St. Joseph, MI, Paper No. 87-2545.

Tang, K. L. 2004 *Soil and Water Conservation in China*. Science Press, Beijing.

Tuset, J., Vericat, D. & Batalla, R. J. 2016 Rainfall, runoff and sediment transport in a Mediterranean mountainous catchment. *Science of the Total Environment* **546**, 114–132.

Vermang, J., Demeyer, V., Cornelis, W. M. & Gabriels, D. 2009 Aggregate stability and erosion response to antecedent water content of a loess soil. *Soil Science Society of America Journal* **73** (3), 718–726.

Wei, W., Jia, F. Y., Yang, L., Chen, L. D., Zhang, H. D. & Yu, Y. 2014 Effects of surficial condition and rainfall intensity on runoff in a loess Hilly area, China. *Journal of Hydrology* **513** (1), 115–126.

Wischmeier, W. H. & Mannering, J. V. 1969 Relation of soil properties to its erodibility. *Soil Science Society of America Journal* **33** (1), 131–137.

Youngs, E. G. 1991 Infiltration measurements – a review. *Hydrological Processes* **5**, 309–320.

Zhao, J. B., Zhang, Y., Chen, B. Q. & Dong, Z. B. 2009 Law of water infiltration of lower part of middle Pleistocene loess in Luochuan of Shaanxi. *Acta Pedologica Sinica* **46**, 965–972.

First received 21 January 2020; accepted in revised form 10 March 2020. Available online 15 April 2020